

Supplementary Information

Near stoichiometric lithium niobate crystal with dramatically enhanced piezoelectric performance for high temperature acceleration sensing

Guoliang Wang^a, Fulei Wang^{b,c}, Xi Gao^a, Dongzhou Wang^{*b,c}, Wei Song^d, Yanlu Li^{*a}, Xueliang Liu^a, Yuanhua Sang^a, Fapeng Yu^{*a} and Xian Zhao^a

^a State Key Laboratory of Crystal Materials, Shandong University, Jinan, 250100, China

^b Jinan Institute of Quantum Technology, Jinan 250101, China

^c Jinan Branch, Hefei National Laboratory, Jinan 250101, China

^d CETC Deqing Huaying Electronics Co., Ltd, Zhejiang 313200, China

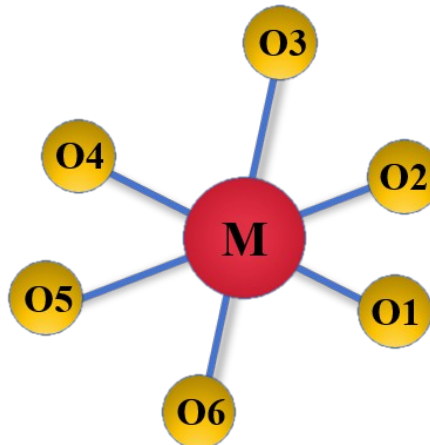


Fig. S1 Distortion model of the MO_6 polyhedron.

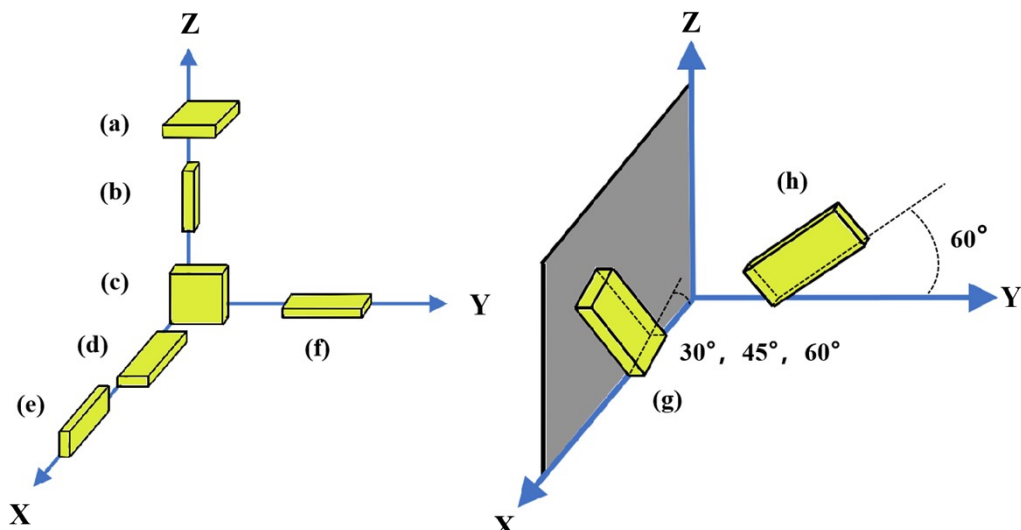


Fig. S2 Crystal cuts for evaluation of the electro-elastic constants [(a) Z-square plate; (b) Z bar; (c) X-square plate; (d) ZX plate; (e) YX plate; (f) ZY plate; (g) YZt/θ ($\theta = 30^\circ, 45^\circ$ and 60°); (h) XYt/θ ($\theta = 60^\circ$)]

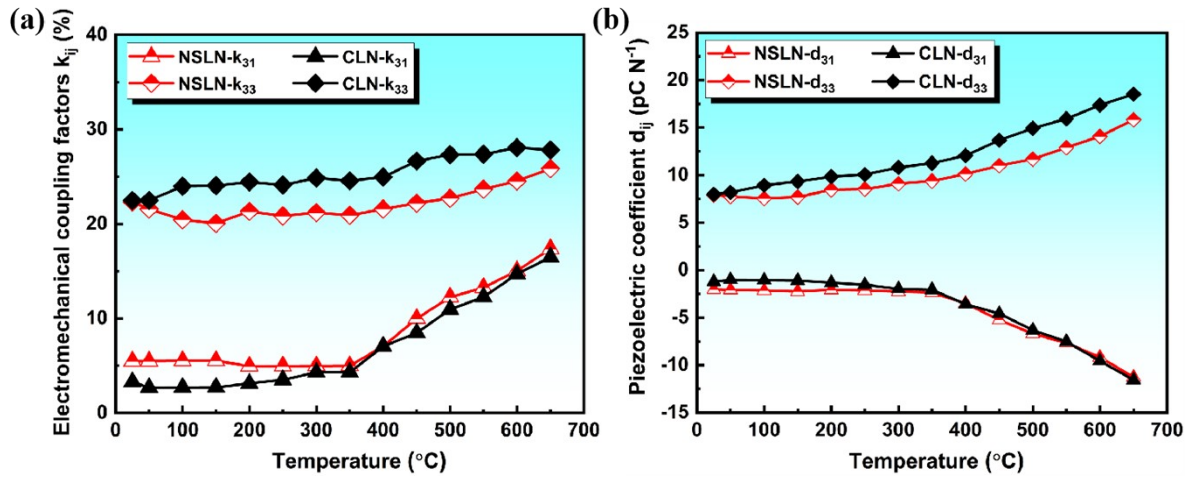


Fig. S3 Variations of (a) electromechanical coupling factors, (b) piezoelectric coefficients as a function of temperatures for NSLN and CLN crystals.

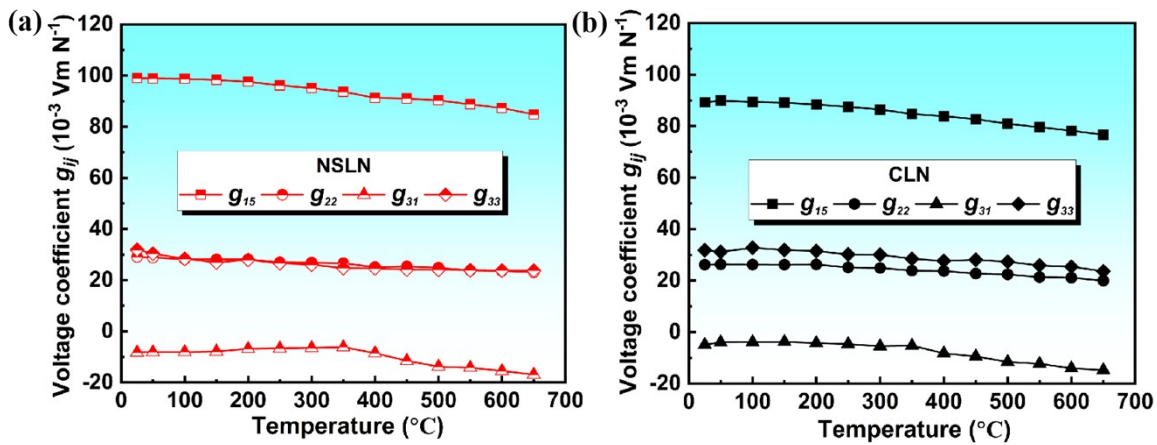


Fig. S4 Variations of piezoelectric voltage coefficients g_{ij} as a function of temperatures for (a) NSLN and (b) CLN crystals.

It was found that the piezoelectric voltage coefficients g_{ij} for NSLN and CLN all showed a decreasing trend with temperature, as shown in Fig. S4. There was a good observation that while the d_{ij} was relatively stable with temperature, the increase in ε_{ij} with temperature leaded to a slight decrease in g_{ij} (since $g_{ij} = d_{ij} / \varepsilon_{ij}$) for NSLN and CLN crystals. Clearly that the g_{15} demonstrated maximum values, which were represented by 98.9×10^{-3} Vm N⁻¹ and 89.2×10^{-3} Vm N⁻¹ for NSLN and CLN crystals at room temperature.

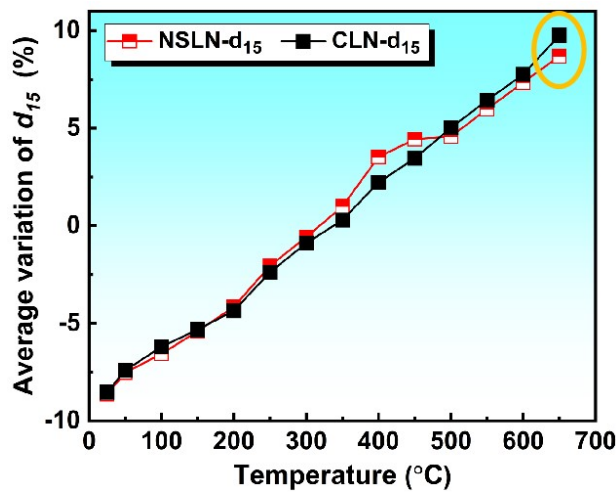


Fig. S5 Average variations of the piezoelectric coefficients d_{15} as a function of temperatures for NSLN and CLN crystals.

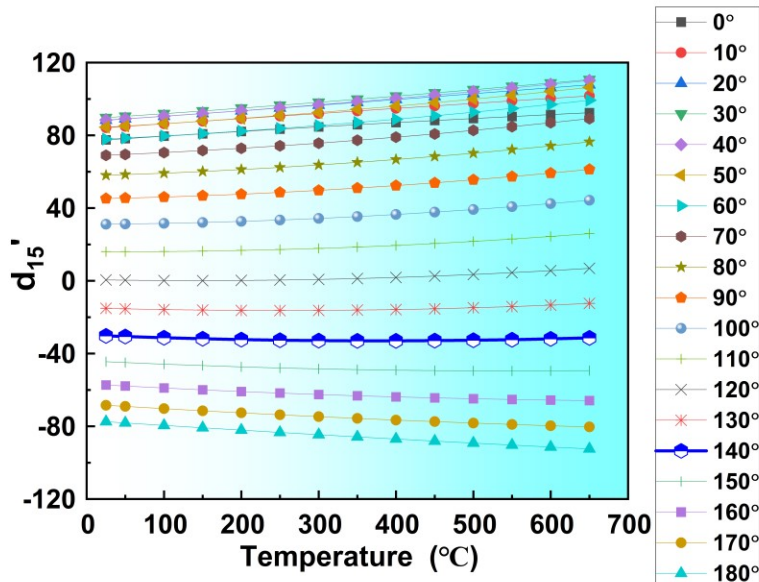


Fig. S6 Variations of the effective piezoelectric coefficients d_{15}' rotated around the X-axis with different angles as a function of temperatures for NSLN crystal.

Table S1 Crystal cuts, vibration modes, material constants and related equations for determination of the electro-elastic constants for NSLN and CLN crystals.

Crystal cuts	Vibration modes	Material constants	Related equations
X plate	/	$\varepsilon_{II}^T / \varepsilon_0$	$\frac{\varepsilon_{ii}^T}{\varepsilon_0} = \frac{C \cdot t}{A \cdot \varepsilon_0}$
Z plate	/	$\varepsilon_{33}^T / \varepsilon_0$	
X plate	thickness shear	d_{15}, s_{55}^E	$k_{ij}^2 = \frac{\pi}{2} \frac{f_r}{f_a} \tan \frac{\pi}{2} \left(\frac{f_a - f_r}{f_a} \right)$ $s_{ii}^E = \frac{I}{4\rho (tf_a)^2 (1 - k_{ii}^2)}$ $d_{ij} = k_{ij} \sqrt{\varepsilon_{ii}^T s_{jj}^E}$
Z bar	longitudinal	d_{33}, s_{33}^E	$k_{ii}^2 = \frac{\pi}{2} \frac{f_r}{f_a} \tan \frac{\pi}{2} \left(\frac{f_a - f_r}{f_a} \right)$ $s_{ii}^E = \frac{I}{4\rho (tf_a)^2 (1 - k_{ii}^2)}$ $d_{ii} = k_{ii} \sqrt{\varepsilon_{ii}^T s_{jj}^E}$
YX plate	length	d_{21}, s_{11}^E	$\frac{k_{ij}^2}{1 - k_{ij}^2} = \frac{\pi}{2} \frac{f_a}{f_r} \tan \frac{\pi}{2} \left(\frac{f_a - f_r}{f_a} \right)$
ZX plate	extension	d_{31}, s_{11}^E	$s_{ii}^E = \frac{I}{4\rho (tf_r)^2}$ $d_{ij} = k_{ij} \sqrt{\varepsilon_{ii}^T s_{jj}^E}$
YZt/ θ		$s_{13}^E \quad s_{12}^E$	$s_{33}^{E'}(\theta) = s_{11}^E \sin^4 \theta + s_{33}^E \cos^4 \theta + (2s_{13}^E + s_{44}^E) \sin^2 \theta \cos^2 \theta$
XYt/ θ		s_{14}^E	$s_{22}^{E'}(\theta) = s_{11}^E \cos^4 \theta + s_{33}^E \sin^4 \theta + (2s_{13}^E + s_{44}^E) \sin^2 \theta \cos^2 \theta - 2s_{14}^E \sin \theta \cos^3 \theta$
			$s_{11}^{E'}(\theta) = s_{11}^E \cos^4 \theta + s_{11}^E \sin^4 \theta + (2s_{12}^E + s_{66}^E) \sin^2 \theta \cos^2 \theta$

Table S2 Distortion Δd of each octahedron contained in the pristine phase and the defect phase.

	Bond	Bond distances (Å)	Bond angle (°)	Δd (Å)
Pristine phase (Nb-O)	Nb ₁ -O ₁	1.90022	165.0362	
	Nb ₁ -O ₄	2.14370		
	Nb ₁ -O ₂	1.90022	165.0376	0.756
	Nb ₁ -O ₅	2.14370		
	Nb ₁ -O ₃	1.90021	165.0349	
	Nb ₁ -O ₆	2.14372		
Pristine phase (Li-O)	Li ₁ -O ₁	2.23463	156.0552	
	Li ₁ -O ₄	2.03026		
	Li ₁ -O ₂	2.23468	156.0533	0.671
	Li ₁ -O ₅	2.03026		
	Li ₁ -O ₃	2.23461	156.0537	
	Li ₁ -O ₆	2.03025		
V_{Li}^- (Nb ₁ -O)	Nb ₁ -O ₁	1.91450	168.9592	
	Nb ₁ -O ₄	2.10781		
	Nb ₁ -O ₂	1.91439	168.9622	0.591
	Nb ₁ -O ₅	2.10751		
	Nb ₁ -O ₃	1.91426	169.0006	
	Nb ₁ -O ₆	2.10761		
(Nb ₂ -O)	/	/	/	0.782
(Nb ₃ -O)	/	/	/	0.713
(Nb ₄ -O)	/	/	/	0.807
(Nb ₅ -O)	/	/	/	0.711
(Nb ₆ -O)	/	/	/	0.807
(Nb ₇ -O)	/	/	/	0.712
(Nb ₈ -O)	/	/	/	0.807
	/	/	/	$\overline{\Delta d}=0.741$
Nb_{Li}^{4+} (Nb _{Li} -O)	Nb _{Li} -O ₁	2.12294	157.1173	
	Nb _{Li} -O ₄	1.92963		
	Nb _{Li} -O ₂	2.12206	157.1548	0.629
	Nb _{Li} -O ₅	1.92955		
	Nb _{Li} -O ₃	2.12309	157.1493	
	Nb _{Li} -O ₆	1.92955		

Table S3 Elastic constants (c_{ij}) and piezoelectric stress constants (e_{ij}) of V_{Li}^- and Nb_{Li}^{4+} calculation models.

c_{ij}	c_{11}	c_{12}	c_{13}	c_{14}	c_{33}	c_{44}	c_{66}
V_{Li}^-	216	74.6	80.7	8.5	239	59.3	69.9
Nb_{Li}^{4+}	223	78.1	81.6	5.5	238	65.9	72
e_{ij}	e_{15}	e_{22}	e_{31}	e_{33}			
V_{Li}^-	4.11	2.12	0.45	1.13			
Nb_{Li}^{4+}	3.31	1.60	0.58	0.97			

Table S4 Concentration of V_{Li}^- and Nb_{Li}^{4+} for LN crystal with different [Li]/[Nb] ratios.

Concentration	NSLN (49.83:50.17)	V_{Li}^- (48.94:51.06)	CLN (48.65:51.35)	Nb_{Li}^{4+} (47.92:52.08)
V_{Li}^- (%)	0.272	1.696	2.160	3.328
Nb_{Li}^{4+} (%)	0.068	0.424	0.540	0.832

Table S5 Bond distances and bond angles for NSLN and CLN crystals. Variations of the distortion Δd of NbO_6 and LiO_6 octahedron for NSLN and CLN crystals.

NSLN				
Bond distances (Å)		Bond angles (°)		Total Δd (Å)
Nb-O ₁	2.1354	$\angle O_1-Nb-O_4$	165.588	0.2812
Nb-O ₄	1.8631			
Nb-O ₂	1.8629	$\angle O_2-Nb-O_5$	165.593	0.2815
Nb-O ₅	2.1356			0.8448
Nb-O ₃	2.1358	$\angle O_3-Nb-O_6$	165.604	0.2821
Nb-O ₆	1.8626			

NSLN				
Bond distances (Å)		Bond angles (°)		Total Δd (Å)
Li-O ₁	2.2566	$\angle O_1-Li-O_4$	153.616	0.2272
Li-O ₄	2.0531			0.6800
Li-O ₂	2.0534	$\angle O_2-Li-O_5$	153.604	0.2266

Li-O ₅	2.2564			
Li-O ₃	2.2562	$\angle O_3-Li-O_6$	153.602	0.0062
Li-O ₆	2.0536			

CLN				
Bond distances (Å)		Bond angles (°)	Δd (Å)	Total Δd (Å)
Nb-O ₁	2.1277	$\angle O_1-Nb-O_4$	165.681	0.2628
Nb-O ₄	1.8731			
Nb-O ₂	1.8731	$\angle O_2-Nb-O_5$	165.681	0.2628
Nb-O ₅	2.1277			0.7884
Nb-O ₃	2.1277	$\angle O_3-Nb-O_6$	165.681	0.2628
Nb-O ₆	1.8731			

CLN				
Bond distances (Å)		Bond angles (°)	Δd (Å)	Total Δd (Å)
Li-O ₁	2.2696	$\angle O_1-Li-O_4$	152.464	0.2479
Li-O ₄	2.0497			
Li-O ₂	2.0497	$\angle O_2-Li-O_5$	152.464	0.2479
Li-O ₅	2.2696			0.7437
Li-O ₃	2.2696	$\angle O_3-Li-O_6$	152.464	0.2479
Li-O ₆	2.0497			

Table S6 Cell parameters for NSLN and CLN crystals.

	NSLN	CLN
Crystal system	Trigonal	Trigonal
Space group	3m	3m
Unit cell dimension (Å)	$a=5.1380(6), c=13.8300(2)$	$a=5.1417(6), c=13.8520(2)$
c/a	2.6917	2.6941
Unit cell volume (Å ³)	316.18	317.14

Table S7 Atomic coordinates for NSLN and CLN crystals.

NSLN			
Atom	x	y	z
Nb ₁	0.66667	0.33333	0.46880
O ₁	0.99192	0.37193	0.36503
O ₂	0.96140	0.67467	0.53165
O ₃	0.62803	0.62004	0.36503

O ₄	0.32529	0.28667	0.53165
O ₅	0.37992	0.00804	0.36503
O ₆	0.71329	0.03856	0.53165

NSLN			
Atom	x	y	z
Li ₁	0.33333	0.66667	0.58200
O ₁	0.65864	0.70527	0.69838
O ₂	0.71333	1.03859	0.53169
O ₃	0.29475	0.95338	0.69838
O ₄	-0.03856	0.67469	0.53169
O ₅	0.04664	0.34138	0.69838
O ₆	0.32533	0.28669	0.53169

CLN			
Atom	x	y	z
Nb ₁	0.66667	0.33333	0.53210
O ₁	0.95213	0.29514	0.63539
O ₂	1.00969	0.62846	0.46870
O ₃	0.70482	0.65696	0.63539
O ₄	0.37151	0.38120	0.46870
O ₅	0.34300	0.04783	0.63539
O ₆	0.61876	-0.00973	0.46870

CLN			
Atom	x	y	z
Li ₁	0	0	0.42000
O ₁	0.28547	-0.03813	0.30204
O ₂	0.37153	0.38125	0.46866
O ₃	0.03815	0.32363	0.30204
O ₄	-0.38122	-0.00968	0.46866
O ₅	-0.32360	-0.28544	0.30204
O ₆	0.00971	-0.37150	0.46866